RSC Advances

PAPER

View Article Online
View Journal | View Issue

Open Access Article. Published on 17 November 2020. Downloaded on 10/27/2025 2:31:16 PM.
This article is licensed under a Creative Commons Attribution-NonCommercial 3.0 Unported Licence.

Check for updates

Cite this: *RSC Adv.*, 2020, **10**, 41791

Advanced bioH_2 and bioCH_4 production with cobalt-doped magnetic carbon

Jishi Zhang,* Wenqian Zhao, Chuanfang Fan, Wenqing Li and Lihua Zang

Received 19th September 2020
Accepted 9th November 2020

DOI: 10.1039/d0ra08013f

rsc.li/rsc-advances

In this work, a novel cobalt-doped magnetic carbon (CDMC) was prepared to boost hydrogen (H_2) and methane (CH_4) generation. A one-pot approach was employed to produce H_2 and CH_4 with an incompletely heat-treated mixed culture. A moderate amount of CDMC promoted biogas evolution, while excess CDMC eroded both H_2 and CH_4 productivity. The CDMC (600 mg L^{-1}) group achieved the highest biogas yields of 176 mL H_2 per g glucose and 358 mL CH_4 per g glucose, which were higher than those (102 mL H_2 per g glucose and 288 mL CH_4 per g glucose) found in the control group without CDMC. The mechanisms of H_2 and CH_4 production *via* the one-pot approach with CDMC were speculated to be as follows: CDMC provided beneficial sites and two elements (Co and Fe) for culture growth and boosted electron transfer, facilitating glucose degradation and conversion. Supplementation of carbon matrix composites and trace elements in biogas production has been shown to be an efficient strategy.

Introduction

To lower global warming and environmental problems due to fossil fuel utilization, various technologies have been developed to produce clean energy.[1] Energy carriers such as biohydrogen and biomethane have been demonstrated to be promising alternatives to fossil fuels. Techniques employed for biogas generation include biological, electrochemical and thermochemical processes. Generally, biological approaches to H_2 and CH_4 generation are related to dark fermentation and photo driven fermentation.[2] Compared to electro- and thermochemical methods, biological techniques have low costs.[3] In addition, dark fermentation is a renewable and nonpolluting process that is more attractive than photo driven fermentation.

To date, dark anaerobic processes have been developed to convert manure, biomass, organic wastewater and sludge into biogas.[1] However, to enhance the overall performance of biogas production, there are still some disadvantages to be overcome, including substrate inhibition and pH fluctuation due to excess organic loads or ammonia accumulation.[1,4] Vu and Min[1] observed that a high amount of glucose (10 g L^{-1}) could cause a lower CH_4 generation rate than other glucose amounts, which was attributed to volatile fatty acid (VFA) suppression. Various strategies for promoting CH_4 evolution and process stabilization have been developed, mainly involving two-pot approaches, pH regulation, conductive material stimulation, electrochemical assistance and trace element addition.[1] Among these methods, conductive material stimulation and trace element addition are simple and practical, and have good research prospects.[5] For the bioH_2 process, the primary bottleneck is the low H_2 yield, which needs to be overcome by optimizing the metabolic pathway. To date, some carbon composites have been shown to boost biogas (*e.g.*, H_2 and CH_4) generation.[6] These carbons can immobilize cultures and boost electron transfer, which facilitate enhanced syntrophic interaction.

Metallic nanoparticles can be immobilized onto the surface of some carbon matrices, such as carbon nanotubes (CNTs), activated carbon (AC), and biochar (BC), as well as their formed carbon composites. The composites improve particle reactivity and decrease particle agglomeration, which can help culture immobilization and cell growth.[6] For instance, an Fe_3O_4/graphene composite increased the H_2 yield by 42%, which contributed to boosting hydrogenase enzymatic activity and accelerating the microbial degradation of organic matter.[7] The highest CH_4 yield from food waste occurred with 75 mg per L Fe_3O_4 particles.[8] Fe_3O_4 is related to iron solubility and bioavailability because soluble iron is an essential factor in biogas evolution and is readily employed by mixed cultures to maintain essential metabolic activities.[6] Previous studies also illustrated that extra Fe_3O_4 could achieve a 20.1–26.4% improvement in bioH_2 yield when a moderate amount of Fe_3O_4 (50–400 mg L^{-1}) was used.[9,10] Han *et al.*[11] found that the H_2 yield from a substrate modified with hematite was increased by 33%. They inferred that hematite could release iron ions to boost the activity of hydrogenase enzymes.[11] Iron-including enzymes are mainly required for the production of H_2. Considering that functional-graphene preparation is complicated and expensive,

College of Environmental Science and Engineering, Qilu University of Technology (Shandong Academy of Science), No. 3501 Daxue Road, Changqing District, Jinan 250353, China. E-mail: lyzhangjishi@163.com

Open Access Article. Published on 17 November 2020. Downloaded on 10/27/2025 2:31:16 PM.
This article is licensed under a Creative Commons Attribution-NonCommercial 3.0 Unported Licence.

employing carbon matrix composites that are relatively easily prepared seems to be a promising method.[12]

Fe, Mn, Co and Ni are essential trace elements that make up cofactors and enzymes. Supplementing anaerobic systems with such elements has been shown to play vital roles in boosting biogas generation.[13–15] Related studies have revealed that an increased biogas yield and lowered VFA inhibition were attributed to some trace metals that exhibited dominant effects in buffering and microbial metabolism during biogas evolution.[14,15] A moderate amount of trace elements improved the assimilative capacity of a mixed culture, improving biogas generation. For instance, Ca, Mg, Co and Ni concentrations of 303.0, 777.0, 7.0, and 3.0 mg L^{-1} have been used.[16] In addition, the inhibition stress from trace elements depends on the salt species and concentration used in anaerobic evolution systems. The availability of trace metals for maintaining microbial growth and metabolism strongly depends on the metal species and chemical states. These factors are also controlled by the total metal amount and other operational parameters. Fe is present in Fe–S clusters, which are associated with culture intracellular reactions. Moreover, Fe participates in oxidase and cytochrome formation.[15] In typical biogas generation systems, Fe is often supplemented at a higher amount than are Co and Ni.[13] Some studies have revealed that a moderate amount of iron, such as Fe^{2+}, Fe_3O_4, Fe^0, and Fe_2O_3, boosted Fe-hydrogenase activity, which caused biomagnification of the H_2 yield.[17,18] In addition, Co can form complexes with soluble metabolic products (SMPs).[13] Co ions in the liquid phase are likely related to vitamin B_{12}, which plays vital roles in methanogenesis.[13] A previous report showed that moderate amounts of Co and Ni ions (0.1–0.3 mg L^{-1}) could be employed to maintain biogas production stability.[13] However, there are few reports on an advanced method for bioH_2 and bioCH_4 production with cobalt-doped magnetic carbon (CDMC) in one bioreactor.

Therefore, the goals of this work are (i) to prepare and characterize CDMC containing Fe, Co and C, (ii) to investigate the effect of CDMC amount on H_2 and CH_4 yields, (iii) to compare the influence of CDMC on microbial morphologies and SMPs, (iv) to elucidate the CDMC promotion effects underlying bioH_2 and CH_4 generation, and (v) to highlight the advantages of the one-pot approach by comparison with previous studies.

Materials and methods

Seed sludge preparation

A seed sludge sample was collected from an anaerobic tank that was used to treat citric acid wastewater and located in Shandong, China. The sludge sample consisted of approximately 15% total solid (TS). The mixed sludge was incubated at 1.0 g per L glucose and 37 °C, which was maintained until biogas generation was accomplished (20 d). Subsequently, the incubated sludge sample was heated at 85 °C for 30 min to select for H_2-generating bacteria (HGB). Then, the sample was cooled to approximately 37 °C and supplemented with 0.5 g per L glucose. The material was cultured at 37 °C for 36 h to obtain a dominant consortium (*e.g.*, HGB). Thus, seed sludge was obtained and used to produce H_2 and CH_4 in one bioreactor. The main characteristics of the seed sludge are shown in Table 1.

CDMC preparation

CDMC was prepared with an alkaline solution under reflux conditions by following the steps below. To obtain Fe^{3+} and Co^{2+} mixed solutions, 5.4944 g of ferric nitrate ($Fe(NO_3)_3 \cdot 9H_2O$) and 1.9790 g of cobalt nitrate ($Co(NO_3)_2 \cdot 6H_2O$) were dissolved in 50 mL H_2O. Subsequently, 24 g AC was intensely mixed with 50 mL alkaline solution containing 3.4 g NaOH at 25 °C for 30 min. The alkaline AC suspension was heated to boiling, and then the mixed solution containing Fe^{3+} and Co^{2+} was rapidly poured into the boiling AC suspension, which was maintained in well-mixed reflux conditions at 115 °C for 120 min. Finally, the suspension was cooled to 35 °C, and solid–liquid separation was achieved. Consequently, the magnetic carbon matrix composite was dried at 80 °C for 12 h and labeled CDMC. Additionally, AC used this work were measured to be 522.56 m^2 g^{-1}. Other chemicals, such as $Fe(NO_3)_3 \cdot 9H_2O$, $Co(NO_3)_2 \cdot 6H_2O$ and NaOH were analytical grade reagent. H_2O was high-purity water that came from a second-level reverse osmosis device located at the Engineering Lab of Light Waste Clean Energy Technology (Shandong, P. R. China).

Anaerobic fermentation design

The bioH_2 generation processes were carried out in a 500 mL bioreactor. The mixed substrates consisted of 0.1 g per L peptone and 10 g per L glucose. Various quantities (0–800 mg L^{-1}) of CDMC were used to prepare 5 concentrations (0, 200, 400, 600 and 800 mg L^{-1}) in a series of bioreactors. Each bioreactor contained 150 mL of anaerobic granular sludge (mixed culture), which was supplemented with a moderate amount of H_2O to reach a volume of 500 mL. The pH values of the reactors was adjusted to 6.9 ± 0.1 by using HCl (0.1 mol L^{-1}) and NaOH (0.1 mol L^{-1}). The moderate headspace (130 mL) of the anaerobic reactor contributed to reducing the H_2 partial pressure. All headspaces were slowly flushed with nitrogen for approximately 40 s to create an anaerobic system. Then, the anaerobic reactors were rapidly sealed by employing a rubber plug connected to two samplers for sampling liquid/gas and a pipe for conveying gas. The generated biogas was collected

Table 1 Seed sludge characteristics

Physicochemical indexes	Seed sludge
pH	6.9 ± 0.1
TS (wt%)	10.5 ± 0.5
VS (wt%)	54.5 ± 0.5
TC (mg L^{-1})	2360 ± 100
TOC (mg L^{-1})	1590 ± 70
IC (mg L^{-1})	800 ± 50
COD (mg L^{-1})	10 600 ± 300
NH_4^+ (mg L^{-1})	2400 ± 100
VFAs (mg L^{-1})	340 ± 10

Open Access Article. Published on 17 November 2020. Downloaded on 10/27/2025 2:31:16 PM.
This article is licensed under a Creative Commons Attribution-NonCommercial 3.0 Unported Licence.

through the gas displacement method. Among the bioreactors, one reactor was not supplemented with CDMC and was used as a control. Finally, all the anaerobic reactors were incubated at 37 °C for 16 d to generate H_2 and CH_4 gases. In addition, the liquid and gas were periodically sampled to investigate the SMP content and the contents of H_2 and CH_4, respectively. All the conditions in the batch experimental designs were tested three times.

Analytical methods

The surface groups, specific surface area, structural morphology and element composition of CDMC were analyzed based on a previous study.[15] The chemical oxygen demand (COD), ammonium (NH_4^+), total solids (TS, wt%) and volatile solids (VS, wt%) contents and pH were determined by following standard analysis methods for water and wastewater.[19] The total organic carbon (TOC, mg L^{-1}) and inorganic carbon (IC, mg L^{-1}) in the liquid phase were measured with a TOC analyzer (TOC-LCPHCN 200, Shimadzu, Japan). As described in a previous report, the distribution and levels of SMPs, such as acetic acid (HAc), propionic acid (HPr), butyric acid (HBu) and ethanol (EtOH), were measured using gas chromatography (GC-2010, Japan) connected with a flame ionization detector.[15] In addition, biogas components (*e.g.*, H_2, CO_2 and CH_4) were determined by another gas chromatograph connected with a thermal conductivity detector (GC-2014C, Japan), whereas the volume of biogas produced was collected by employing a gas displacement technique. The injector and detector were controlled at 150 °C and 180 °C, respectively. Prior to microbial observation, the culture immobilization was performed, as shown in a previous work.[15] The morphologies of mixed cultures in the control and CDMC groups were observed with an emission scanning electronic microscope (SEM, Supra-55, Germany). To confirm the magnetic property of NDMC, its pattern was determined *via* a vibrating sample magnetometer (VSM, SQUID-MPMS3, USA) at room temperature.

Kinetic description

The major parameters of anaerobic reaction kinetics can significantly affect various physicochemical and biological factors. The highest biohydrogen yield (HHY) and the highest methane yield (HMY) were estimated using the experimentally determined cumulative biogas yield. Lag time (λ), HHY and HMY are vital parameters that indicate the overall performance of biogas production system. Furthermore, these kinetic parameters were calculated according to the modified Gompertz and logistic equations, as presented in eqn (5) and (6), respectively.[15]

$$Y(t) = Y_m \exp\left\{-\exp\left[\frac{R_m e}{Y_m}(\lambda - t) + 1\right]\right\} \quad (1)$$

$$Y(t) = Y_m \Big/ \left\{1 + \exp\frac{4R_m}{Y_m}(\lambda - t) + 2\right\} \quad (2)$$

Here, $Y(t)$ describes the cumulative biogas yield (mL H_2 per g glucose (t, h) or mL CH_4 per g glucose (t, d)), R_m is associated with the highest biogas yield rate (mL H_2 per g glucose per h or mL CH_4 per g glucose per d), Y_m represents the HHY or HMY (mL), λ is related to the lag time (h or d), and e is 2.72. Y_m, R_m, and λ in the two equations were estimated by using the software Origin 8.5, and the correlation coefficient (R^2) values were investigated. These kinetic parameters are useful to understand the dynamics and some underlying mechanisms of the anaerobic process.

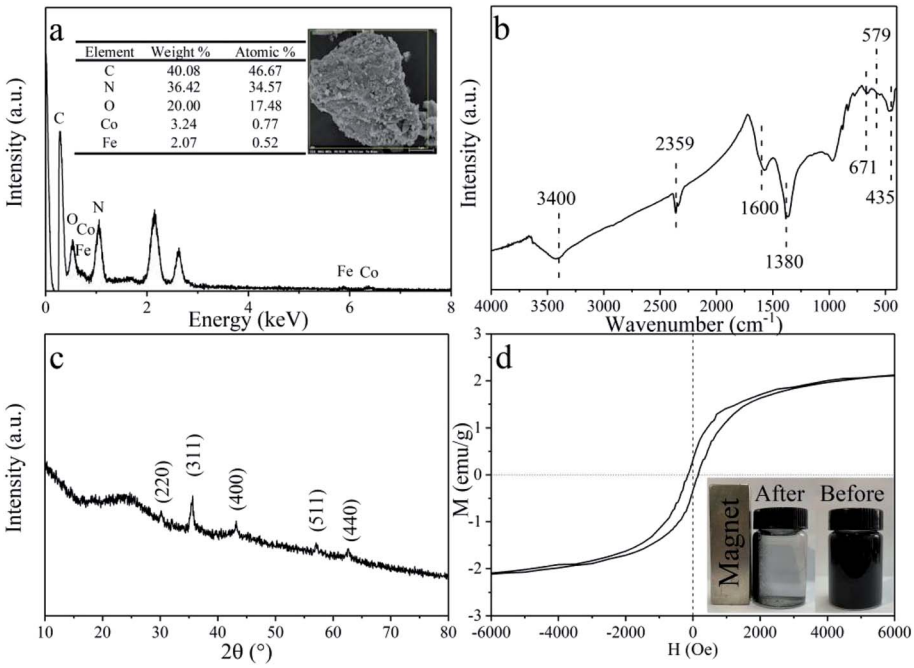

Fig. 1 CDMC characteristics according to SEM/EDS (a), FT-IR (b), XRD (c) and VSM (d).

Open Access Article. Published on 17 November 2020. Downloaded on 10/27/2025 2:31:16 PM.
This article is licensed under a Creative Commons Attribution-NonCommercial 3.0 Unported Licence.

Results and discussion

Characterization of the CDMC sample

The specific surface area of the CDMC composite is 105.3 m^2 g^{-1}, according to the Brunauer–Emmett–Teller (BET) method. Both the morphology and elemental composition of CDMC are also revealed in Fig. 1a. As shown in Fig. 1a, $CoFe_2O_4$ is scattered and inlayed into the granular AC. The atomic composition of CDMC includes 46.67%, 17.48%, 0.77% and 0.52% C, O, Co and Fe, respectively. In addition, a certain amount (34.57%) of N is present in CDMC, which is likely due to the feedstocks employed during the CDMC preparation process. Similarly, two noteworthy bands occurred at 1.0 keV and 2.1 keV, which are associated with Na and Au, respectively. These phenomena are likely attributed to the utilization of NaOH and Au in the CDMC preparation and detection processes.[15] In addition, the chemical groups on the surface of the CDMC sample were measured using Fourier transform infrared (FTIR) spectroscopy, and the results are revealed in Fig. 1b. Some featured bands of the CDMC sample are as follows: the peaks near 3400 cm^{-1} and 1600 cm^{-1} are related to –OH stretching vibration bands originating from H_2O and $Fe(OH)_3$, respectively. The peak at 435 cm^{-1} is associated with goethite α-FeOOH vibrations.[20] The peak located at 1380 cm^{-1} is attributed to $-NO_3$ vibrations. The peak located at 671 cm^{-1} is related to Co–O stretching vibrations from $Co(OH)_2$. In addition, the band at 2359 cm^{-1} is related to the stretching vibrations of oxygen-containing groups, such as –COOH, on the surface of the CDMC composite. The unique structure of the composite is mainly associated with the presence of $CoFe_2O_4$ in CDMC, whose band can be observed at 579 and 530 cm^{-1}.[15,21] On the other hand, XRD characterization result shows that CDMC has typical graphite characteristics. When the value of 2θ is in the range of 20–30°, a large and wide peak appears, which is related to (002) graphite plane. In addition, the characteristic diffraction peaks observed at 30.12°, 35.63°, 43.19°, 57.05° and 62.60° correspond to the (220), (311), (400), (511) and (440) crystalline planes of the $CoFe_2O_4$ structures (JCPDS card no. 22-1086).[21] Thus, the qualitatively physical phase identification by XRD indicates that $CoFe_2O_4$ is successfully doped on AC. Moreover, the saturation magnetization, residual magnetization and coercive force of CDMC were 2.12 emu g^{-1}, 0.32 emu g^{-1}, and 149.95 Oe (Fig. 4d). CDMC showed good magnetic response when exposed to an external magnet and could be collected quickly from the liquid phase (Fig. 1d).

Effects of CDMC on bioH_2 and bioCH_4 generation

Theoretically, 1 mole of glucose can produce 12 moles of H_2 and 6 moles of CO_2 (eqn (3)). However, from a practical point of view, 1 mole of glucose can produce xCO_2 and 2–4 moles H_2, along with SMPs. Significant differences of the SMPs distribution indicate that the anaerobic metabolic pathways are controlled by dominant microorganisms. During the process of microbial community evolution, the dominant anaerobes depend strongly on the mixed culture source, conductive materials and operational parameters, such as the process pH, fermentation temperature, H_2 partial pressure, substrate components and organic loading rate (OLR), as well as conductive composites and their levels[22,23]

$$C_6H_{12}O_6 + 6H_2O \rightarrow 6CO_2 + 12H_2 \quad (3)$$

Biohydrogen evolution involves a complex pathway, and the components and distribution of SMPs mainly depend on the species and quantities of microorganisms employed in the bioevolution process under the same operating parameters. SMP generation also contributes to bioH_2 evolution under conditions controlled by dominant microbes. In addition, either mixed or single cultures are employed to convert glucose to mixed gases, such as H_2, CH_4 and CO_2.[2] CDMC supplementation increases interspecies hydrogen transfer (IHT) and decreases the spatial distance between different members from the mixed culture consortium growing on some substrates, which are beneficial for degrading glucose, producing VFAs, and converting them into biogas.

To determine the organic load obtained with CDMC, the pH of the batch anaerobic system was not regulated. During the initial period of the fermentation process, H_2 accumulation occurred in the control group compared with the H_2 content in the CDMC reactors (Fig. 2a). This indicated the anaerobes were better adapted to use the substrate at CDMC concentrations between 200 and 800 mg L^{-1}. Fig. 2a shows that H_2 production

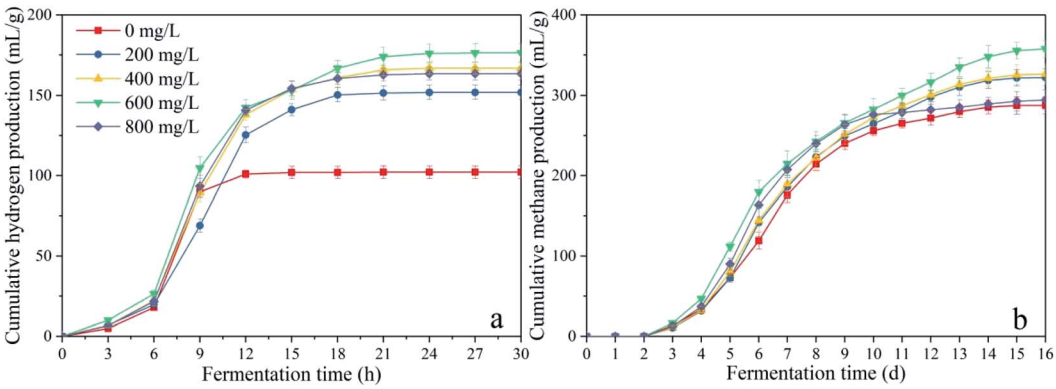

Fig. 2 Impacts of CDMC concentration on (a) H_2 and (b) CH_4 yields.

Open Access Article. Published on 17 November 2020. Downloaded on 10/27/2025 2:31:16 PM.
This article is licensed under a Creative Commons Attribution-NonCommercial 3.0 Unported Licence.

occurred in the earlier stage (48 h), which accompanied by VFA and ethanol generation. As presented in Fig. 2a, an increase in H_2 yield was also achieved at various concentrations of CDMC. When the CDMC concentration was raised to 600 mg L^{-1}, the highest H_2 yield was observed to be 176 mL H_2 per g glucose, which was 72.5% higher than that found in the control group without CDMC addition (102 mL H_2 per g glucose). Fig. 2a also illustrates that excess CDMC (*e.g.*, 800 mg L^{-1}) erodes H_2 productivity, which is probably due to the toxicity to microbes caused by extra CDMC.

On the other hand, the bioH_2 process lasted until H_2 production was accomplished (48 h). CH_4 generation occurred on the 3rd day because some anaerobic culture consortia, such as methanogens (*Methanobacterium* and *Methanosaeta*) and thermoacidophiles were not completely inhibited in the pre-heating treatment step.[24] Moreover, the culture consortia were gradually activated through stimulation by Co ions from CDMC. These microbes probably take part in CH_4 generation through the following two reactions (eqn (4) and (5)):

$$CH_3COOH \rightarrow CO_2 + CH_4 \quad (4)$$

$$4H_2 + CO_2 \rightarrow 2H_2O + CH_4 \quad (5)$$

During the acetoclastic methanogenesis process, acetate (CH_3COOH) is converted by acidophiles to CO_2 and CH_4. Meanwhile, hydrogenotrophic methanogens use H_2 and CO_2 as substrate to produce CH_4 and H_2O. According to these reactions, with prolonged fermentation time, the methanogens were activated and adapted to the environment caused by CDMC introduction. Methanogens replaced HGB and became the dominant microbes, which led to a decreasing H_2 yield and increasing CH_4 yield. Moreover, the CH_4 yield increased as the CDMC content was increased from 0 to 600 mg L^{-1}. The 600 mg per L CDMC group achieved the highest yield of 358 mL CH_4 per g glucose, which was 24.3% more than that observed in the control reactor (288 mL CH_4 per g glucose). A similar study was conducted by Abdelsalam *et al.*[25] who found that the overall performance of the bioCH_4 generation process was improved by supplementing Co and Ni and that a small amount of nanoparticles, such as Co, Ni, Fe and Fe_3O_4, boosted the CH_4 yield by up to 1.7-fold.[25] In addition, CDMC promoted TOC decomposition and its conversion into biogas, resulting in a reduction in TOC concentration (Fig. 3). Interestingly, the group with 600 mg per L CDMC achieved higher methane content than the control group, while the ammonia nitrogen concentration did not increase significantly (Fig. 3). This reduced the inhibition of ammonia on the activity of methane synthase.[26] CDMC has a porous structure, which offers a good environment for both the colonization and metabolism of syntrophic anaerobes growing on the cosubstrate. Such interactions boosted TOC degradation and biogas evolution.[27]

Besides, the data of biohydrogen and biomethane production were analyzed by the one-way ANOVA using IBM SPSS Statistics 22 to determine whether CDMC had a significant effect on them. Statistical significance was delimited by *p*-values equal or less than 0.05.[28] The detailed statistical analysis results

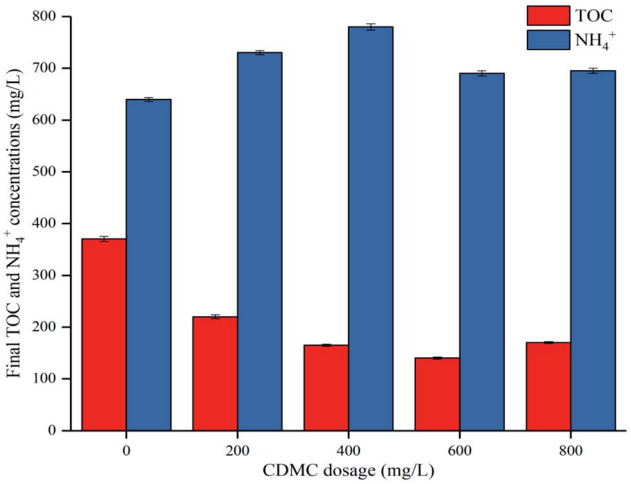

Fig. 3 Impacts of CDMC dosage on final TOC and NH_4^+ concentrations.

were shown in Table 2. It can be seen that the *p*-values of the biohydrogen and biomethane yields are both less than 0.001. This indicated that the addition of CDMC could significantly affect the performance of dark fermentation and anaerobic digestion process, whose mechanisms will be further explained in next section.

As shown in Fig. 2b, excess CDMC (*e.g.*, 800 mg L^{-1}) obviously eroded H_2 and CH_4 productivity. The aforementioned phenomena could likely be attributed to the following aspects: (i) excess CDMC could aggregate, which decreased mass transfer and SMP conversion; (ii) excess CDMC could penetrate the cell wall and cause oxidative stress, which inhibited anaerobes;[15] and (iii) excess CDMC (800 mg L^{-1}) could elevate the final pH (7.9) and increase free ammonia (NH_3–N) generation, which would limit microbial activity.[29] In addition, anaerobic digestion using a one-pot approach combined with CDMC could achieve *in situ* CO_2 sequestration to elevate the CH_4 content.[6] Fe^{2+} from Fe^{3+} reduction was also observed to be metabolized by microbial activity, which boosted the capture of CO_2 and converted CO_2 and H_2 to CH_4.[30]

Effects of CDMC on SMPs

The data in Fig. 4 show that CDMC could also affect the SMP distribution and content during biogas production. The SMPs consisted of EtOH and VFAs such as HBu, HAc, and HPr. As described in eqn (6)–(8), the main metabolic pathways of bioH_2 evolution included EtOH, HAc and HBu pathways.

Table 2 One-way ANOVA on H_2 and CH_4 yields

		DF	MS	*F*	*p*-Value
H_2 yield	Between groups	4	2579.139	551.098	<0.001
	Residual	10	4.680		
	Total	14			
CH_4 yield	Between groups	4	2248.863	72.128	<0.001
	Residual	10	31.179		
	Total	14			

Open Access Article. Published on 17 November 2020. Downloaded on 10/27/2025 2:31:16 PM.
This article is licensed under a Creative Commons Attribution-NonCommercial 3.0 Unported Licence.

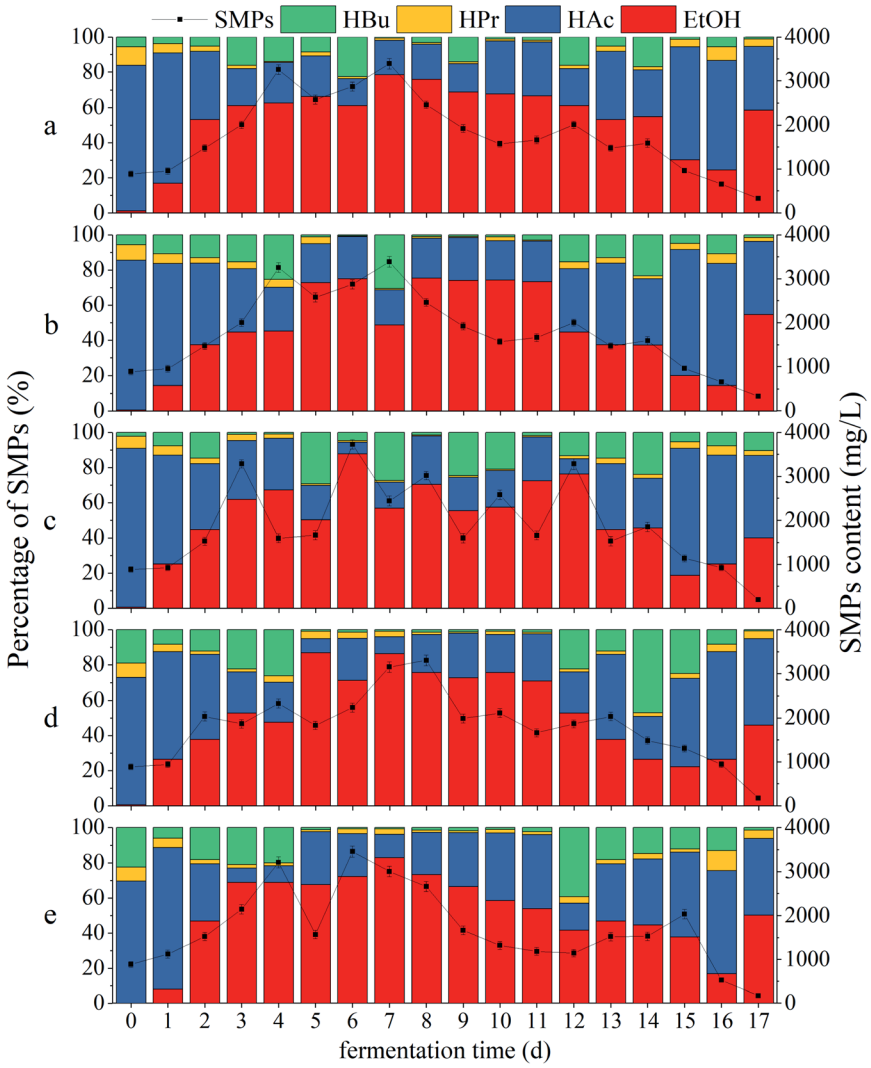

Fig. 4 Impacts of CDMC dosage on SMP concentration and distribution: (a) control (0 mg per L CDMC), (b) CDMC (200 mg L^{-1}), (c) CDMC (400 mg L^{-1}), (d) CDMC (600 mg L^{-1}), and (e) CDMC (800 mg L^{-1}).

$$C_6H_{12}O_6 + 2H_2O \rightarrow 2CH_3COOH + 2CO_2 + 4H_2 \quad (6)$$

$$C_6H_{12}O_6 \rightarrow C_3H_7COOH + 2CO_2 + 2H_2 \quad (7)$$

$$C_6H_{12}O_6 + 2NADH + 2H_2O \rightarrow 2CH_3CH_2OH + 2HCO_3^- + 2NAD^+ + 2H_2 \quad (8)$$

Fig. 4 reveals that all the ratios of (HAc + EtOH)/SMPs exceeded 70%, which indicated that EtOH-type evolution was dominant in the bioH_2 generation process (Fig. 4).[31] The moderate amount of VFAs caused a suitable pH of 4.5–6.0; such pH values facilitated to provide desirable conditions for H_2-producing microbes, thereby increasing the H_2 yield.[32] The HAc concentration gradually increased with increasing CDMC concentration from 0 to 600 mg L^{-1} (Fig. 4). During the bioH_2 generation phase, the feedstock with 600 mg per L CDMC achieved the highest contents of HAc and SMPs, which were 982 mg L^{-1} and 2033 mg L^{-1}, respectively (Fig. 4d). However, the HAc and SMP concentrations decreased significantly when the CDMC concentration exceeded 600 mg L^{-1}, particularly when the CDMC concentration was further raised to 800 mg L^{-1}. In addition, when the NADH-consuming pathways, such as those related to EtOH and HPr metabolism, could be inhibited by controlling the operational parameters, bioH_2 productivity through the NADH oxidation pathway was boosted (eqn (8)). Moreover, the concentration of CDMC could also impact the H_2 yield, whose changes were consistent with SMP concentration and distribution (Fig. 2a). Vu and Min observed that HAc or HPr was dominant in acidogenic products in bioreactors loaded with 2 and 4 g per L glucose, whereas HBu dominated among VFAs at a high OLR of 10 g per L glucose.[1] Similar work was performed by Zheng *et al.*[33] who concluded that the VFA components and distribution were dependent on the system pH level in the bioH_2 evolution process. HAc generation generally occurred under neutral conditions or at a moderate amount pH (6.0–8.0), while a low pH (4.0–5.0) helped generate HBu.[33]

Open Access Article. Published on 17 November 2020. Downloaded on 10/27/2025 2:31:16 PM.
This article is licensed under a Creative Commons Attribution-NonCommercial 3.0 Unported Licence.

VFAs are the major intermediates during the bioCH_4 process. Moreover, CH_4 generation occurred with prolonged time when some methanogens, such as acetoclastic and hydrogenotrophic methanogens, were activated by the stimulation of Fe^{2+} and Co^{2+} ions from extra CDMC and became dominant in microbial succession. Consequently, the H_2 yield was reduced, whereas the CH_4 yield was obviously increased, because hydrogenotrophic methanogens could consume H_2 to produce CH_4. This result was similar to a previous study, in which an optimal time between 36 h and 48 h for bioH_2 production with a mixed culture was observed by Satar *et al.*[2] During the subsequent bioCH_4 process, similar VFA and SMP concentrations were present in all cases (Fig. 2). In addition, synergetic microbes can achieve direct interspecies electron transfer (DIET).[6] For instance, the electrons generated by *Geobacter* during EtOH conversion to bioCH_4 were transferred to other cultures, such as *Methanosarcina* and *Methanosaeta* methanogens, through c-type cytochrome or conductive pili for CH_4 evolution *via* the pathway of CO_2 reduction (eqn (5)).[34] A previous report demonstrated that either adopting EtOH-type evolution or feeding EtOH was a feasible strategy for obtaining large quantities of *Geobacter* and boosting DIET-based synergetic communities. When EtOH was absent from the SMPs, IHT-based methanogens were dominant in methanogenic communities and could completely replace DIET-based methanogens.[35] Interestingly, as shown in Fig. 2, the presence of EtOH could achieve the gradient utilization of SMPs to obtain more biogas. Although CH_4 generation was closely associated with the SMP concentration and composition, EtOH could not be directly converted into CH_4. Moreover, the acetogens consuming EtOH were slightly inhibited during subsequent CH_4 production under weak alkalinity.[36] In the bioCH_4 production phase, as the evolution time increased, SMPs gradually began to decline at 7 d, while the EtOH concentration obviously decreased from 13 d. The final SMP concentration ranged from 500 to 900 mg L^{-1}, whereas HAc accounted for approximately 50% of SMPs in all cases. However, EtOH degradation in the bioCH_4 evolution process was not obvious because there were not enough acetogenic microbes to convert EtOH to HAc. In addition, CH_4 generation was slower at the high CDMC concentration of 800 mg L^{-1} than at other concentrations, likely due to the low degradation of EtOH. Therefore, the SMP distribution in the liquid effluent from the bioprocess varied slightly due to differences in CDMC concentration and microbial diversity.

Impacts of CDMC on microbial morphologies

Fe^{3+} reduction to Fe^{2+} through mixed cultures is a beneficial electron sink for oxidizing HAc in the initial stage of methanogenesis, which diverts the electron flow from CH_4 generation.[37] However, only a small amount of Fe_3O_4 introduced by CDMC took part in Fe^{3+} reduction, since Fe_3O_4 has low solubility. In addition, a large amount of Co^{2+} was released from the CDMC material and boosted the activity of methanogens. Consequently, methanogens became the dominant electron-accepting microbes after the Fe^{3+} reduction process. Methanogenic archaea are present at the end of the microbial chain in anaerobic systems since they are direct producers of CH_4 and can directly convert HAc or H_2/CO_2 into CH_4. One-reactor streamlined the process and achieved the degradation and conversion of glucose using HGB and methanogens. Moreover, CDMC boosted the DIET between HGB and electrotrophic methanogens.[38]

The microbial morphologies in the final stages of the control and CDMC (600 mg L^{-1}) groups are shown in Fig. 5. Compared with the control reactor (Fig. 5a), the number of anaerobes in the CDMC group (600 mg L^{-1}) illustrated obvious enrichment (Fig. 5b). In addition, the stimulation of anaerobes by CDMC intervention evidently caused the secretion of extracellular polymeric substances (EPS). A previous study revealed that proteins were dominant in EPS, followed by polysaccharides.[39] Surface EPS could be related to both interspecies electron and mass transfer.[39] Zhao *et al.* examined granular sludge in methanogenic tanks fed with SMPs from ethanol-type evolution and observed high conductivity for DIET.[40] They found that *Geobacter* species such as *G. metallireducens* and *G. sulfurreducens* facilitated DIET through their e-pili to form culture aggregates.[38] Moreover, coccus-shaped bacteria were present in the control experiment, while rod-shaped microbes were dominant in the CDMC (600 mg L^{-1}) group (Fig. 5). Guo *et al.*[41] investigated an interesting phenomenon in which short rod-shaped cells of *Pseudomonas* sp. GZ1 grew well at 35 °C but could still survive when treated at 80 °C for 120 min. This phenomenon indicated that strain GZ1 was capable of converting some nutrients, such as carbohydrates and proteins, into acetate and simultaneously obtaining H_2. Satar *et al.*[2] employed an immobilized mixed-culture system to produce H_2 and CH_4 with glucose. They found that the mixed cultures could consume more glucose to generate H_2 and CH_4 at 60 °C than at other temperatures.[2]

Rod-shaped cultures constituted the dominant communities and were capable of producing higher CH_4 yields than those obtained from communities dominated by coccus-shaped bacteria. Consequently, a moderate amount of CDMC (200–600 mg L^{-1}) had a positive impact on both bacteria and archaea that were prominently promoted, such as *Geobacillus* sp., *M. thermophilus*, *M. defluvii*, and *T. thermosaccharolyticum*, which led to a high CH_4 yield.[42] In addition, humic substances, such as humic and fulvic acids, have been found to be electron mediators that could boost long-distance DIET in syntrophic cultures.[43] Thus, CDMC selectively achieved functional

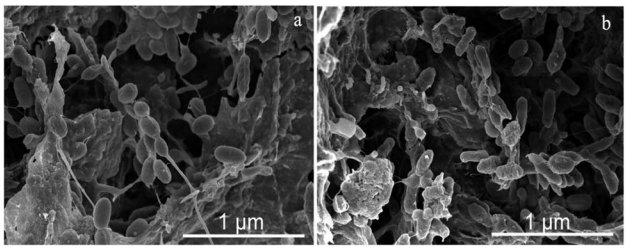

Fig. 5 Microbial morphology in final phases: (a) control and (b) CDMC (600 mg L^{-1}).

Open Access Article. Published on 17 November 2020. Downloaded on 10/27/2025 2:31:16 PM.
This article is licensed under a Creative Commons Attribution-NonCommercial 3.0 Unported Licence.

microbial colonization with rod-shaped bacteria, and served as the H^+/CH_3^+ transfer medium during anaerobic digestion process. However, the microbial diversity and the culture of rod-shaped and coccus-shaped microbes also depended on the anaerobic culture, substrate components, OLR, pH level, and process temperature. The environmental variables of SMPs and pH have strong impacts on microbial community structure. pH is a vital abiotic factor that affects the survivals of different microbes, rate of biological reaction, and energy production.[44] The end pH levels in all digesters were 7.2–7.9, higher than those in the initial stages (6.9). Excess CDMC caused a high final pH value. In addition, the free NH_3, Fe^{2+}, and Co^{2+} concentrations had direct impacts on the overall pH and the dominant microbial community of the anaerobic system.[45] However, excess CDMC could cause oxidative stress harm, which eroded the bacterial cell membrane and limited key enzymatic activity. Thus, the relationship between parameter fluctuations and microorganisms could reasonably explain the above problems.

Kinetic evaluation

As shown in Tables 2 and 3, the main dynamic parameters, such as Y_m, R_m and λ, were calculated by using the experimentally determined cumulative H_2 and CH_4 yields and fitting to eqn (1) and (2), which are the modified Gompertz and logistic equations, respectively. These results indicate that good curve fittings to the experimental data were obtained with the two equations, with relatively high R^2 levels (over 98%). As demonstrated in Tables 2 and 3, the lag times of both bioH_2 and CH_4 generation in the one-pot process for the CDMC groups were 4.63–7.70 h and 2.84–3.80 d, respectively. The values were consistent with previous studies that found lag times of 4.8–7.3 h and 9.52–9.76 h for bioH_2 processes modified with Fe_2O_3 and AC, respectively.[31,46] Tables 2 and 3 reveal that the lag times of the CDMC groups were similar to those observed in the control group. The results were possibly affected by the process pH, sludge community and OLR. Chen *et al.*[47] concluded that a moderate pH could reduce lag time and be useful for H_2 generation by acclimated anaerobes. Moderate pH values between 6.5 and 7.0 facilitated the production of H_2.[47] Furthermore, pH values of 7.0–7.5 were the best for enhancing CH_4 production.[6] In this study, the pH in biogas production ranged from an initial value of 6.9 to a final value of 7.9 (data not shown), which indicates that such pH levels could be beneficial for biogas production. This relationship suggests that some anaerobes could acclimate to the environmental changes introduced by CDMC and become dominant microorganisms.

In addition, Table 3 illustrates that the highest values of Y_m (H_2) (174.02 and 171.78 mL H_2 per g glucose) occurred at 600 mg per L CDMC; these values were obtained using the modified Gompertz and logistic equations, respectively. The two values were slightly lower than those (210.51 and 209.90 mL H_2 per g glucose) determined for a mesophilic H_2 process modified with 400 mg per L manganese-doped magnetic carbon (MDMC).[15] The Y_m (H_2) values were positively correlated with CDMC concentrations ranging from 0 to 600 mg L^{-1} and corresponded to the highest R_m (H_2) values of 22.83 and 22.33 mL g^{-1} h^{-1} (Table 3). Similarly, the CDMC group (600 mg L^{-1}) obtained the highest Y_m (CH_4) values of 355.73 and 343.68 mL CH_4 per g glucose, which were fitted with the modified Gompertz and logistic equations, respectively (Table 4). Surprisingly, the Y_m (CH_4) values were in proportion to the CDMC concentration up to 600 mg per L CDMC, and the corresponding R_m values were 50.08 and 50.59 mL g^{-1} d^{-1}. The two kinetic equations also illustrated that the microbial growth curves for bioH_2 and CH_4 production demonstrated sigmoidal trends that had positive correlations with the H_2 and CH_4 yields.

Table 3 Kinetic values fitted by the Gompertz and logistic equations of H_2 evolution

CDMC (mg L^{-1})	Gompertz equation				Logistic equation			
	Y_m (mL g^{-1})	R_m (mL (g h)$^{-1}$)	λ (h)	R^2 (%)	Y_m (mL g^{-1})	R_m (mL (g h)$^{-1}$)	λ (h)	R^2 (%)
0	102.02	32.99	5.49	99.84	101.97	29.73	5.59	99.88
200	152.89	21.16	5.48	99.68	151.31	20.91	5.7.0	99.91
400	166.22	23.60	5.16	99.86	164.53	23.11	5.32	99.73
600	174.02	22.83	4.63	99.32	171.78	22.33	4.75	99.00
800	163.21	25.70	5.28	99.79	161.82	25.21	5.44	99.79

Table 4 Kinetic values fitted by the Gompertz and logistic models of CH_4 evolution

CDMC (mg L^{-1})	Gompertz equation				Logistic equation			
	Y_m (mL g^{-1})	R_m (mL (g d)$^{-1}$)	λ (d)	R^2 (%)	Y_m (mL g^{-1})	R_m (mL (g d)$^{-1}$)	λ (d)	R^2 (%)
0	288.73	51.97	3.57	99.93	282.13	53.01	3.8	99.75
200	323.24	51.45	3.45	99.78	313.96	52.76	3.67	99.14
400	327.75	51.47	3.38	99.84	318.39	52.07	3.61	99.21
600	355.73	50.08	2.84	99.34	343.68	50.59	3.07	98.27
800	291.27	64.29	3.51	99.93	286.88	64.39	3.67	99.68

Open Access Article. Published on 17 November 2020. Downloaded on 10/27/2025 2:31:16 PM.
This article is licensed under a Creative Commons Attribution-NonCommercial 3.0 Unported Licence.

When CDMC concentrations exceeded 600 mg L^{-1}, continuing to increase the amount of CDMC decreased the Y_m values (H_2 and CH_4), which indicated that excess CDMC could erode bacterial activity. Excess CDMC caused oxidative stress and free NH_3–N inhibition, leading to toxicity. The samples supplemented with 40–60% carbon composites were nontoxic to anaerobes that were present in the H_2 evolution process, but excess metallic ions possibly eroded the microorganisms when large amounts of CDMC were employed. Moreover, the cytotoxicity probably came from the higher final pH (7.9) at 800 mg per L CDMC, which could shift the NH_4^+–N and NH_3–N dissociation equilibrium toward NH_3–N evolution.[29] NH_3–N is regarded as a critical factor of toxicity because of its high permeability *via* cell membranes,[29] which causes K^+ depletion and intracellular proton imbalance.[26] NH_3–N restriction commonly occurs in thermophilic anaerobic digestion.[48] Nevertheless, some ions, such as Co^{2+} and Fe^{2+}, derived from the CDMC composite could take part in the acid–base equilibrium of the anaerobic system (eqn (9)–(11)), in which VFAs are represented by C_xH_yCOOH.[6]

$$NH_4^+ + OH^- \rightarrow NH_3 \cdot H_2O \quad (9)$$

$$CO_2 + H_2O \rightarrow HCO_3^- + H^+ \quad (10)$$

$$C_xH_yCOOH + NH_3 \cdot H_2O \rightarrow C_xH_yCOO^- + NH_4^+ + H_2O \quad (11)$$

However, excess CDMC led to more Co^{2+} and Fe^{2+}, which disturbed the acid–base balance, thereby causing an excess liquid pH. The high pH level led to excess NH_3, which could significantly limit microorganisms. Luo *et al.*[27] and Park *et al.*[49] observed that a system with AC maintained steady CH_4 generation regardless of NH_4^+–N and acid stress but an increase in CH_4 yield could not be achieved with AC alone. It is possible that *Geobacter* species participate actively in DIET, employing VFAs, EtOH and H_2 as major electron acceptors.[49] Moreover, DIET is faster than IET through H_2 for CH_4 formation.[49] Zhang *et al.*[50] concluded that BC supplementation in anaerobic digestion improved the growth of *Methanosarcina* compared with H_2-consuming bacteria (eqn (5)), being in accordance with the higher CH_4 yields in BC-amended bioreactors in comparison to other bioreactors without BC. Gustavsson *et al.*[13] confirmed that Ni or Co was a key element for maintaining bioCH_4 generation process stability and boosted the substrate utilization level. In addition, Co^{2+} is related to vitamin B_{12}, which is present as Co corrinoids. Enzymes containing B_{12} dominate in the methanogenesis process, which enables methanogens to excrete B_{12} compounds into liquid stage.[39]

Comparison with similar studies

As summarized and compared in Tables 4 and 5, some studies have reported carbon or metal composites that can boost bioCH_4 and H_2 production. The enhancements in CH_4 and H_2 yields were closely dependent on the substrate level and other operational parameters. The highest H_2 yield in this work was 176 mL per g glucose, which was higher than those (83–148 mL per g glucose) previously reported by some researchers[15,17,18] and lower than those (211.55–234.4 mL per g glucose) previously reported by others (Table 5).[15,22,51,52] In addition, the highest increase in experimental CH_4 yield was 24.3%, which was similar to that determined by Lin *et al.* (25%),[53] and lower than those found by Luo *et al.*[27] (70.6%),

Table 5 Similar studies using different carbons in bioH_2 production

Anaerobic seed	Carbon (mg L^{-1})	Temp. (°C)	Initial pH	H_2 yield (mL per g glucose)	Reference
Heated sludge	MDMC (400)	37	6.8	211	15
Heated sludge	MDMC (600)	55	6.9	148	15
Mixed culture	AC (—)	37	4.0	144.36	17
Heated sludge	Fe^0/AC (400)	30	7.0	83.34	18
Heated sludge	Fe_2O_3/CNPs (300)	37	6.6	218.63	22
Mixed culture	AC (—)	37	5.5	211.55	51
Heated sludge	Fe^{2+}/BC (200/600)	37	6.8	234.4	52
Heated sludge	CDMC (600)	37	6.9	176	This study

Table 6 Similar studies using different carbons in bioCH_4 production

Anaerobic seed	Carbon (g L^{-1})	Substrate	Temp. (°C)	HRT (d)	Increase in CH_4 yield (%)	Reference
Mixed culture	BC (10)	Glucose	35	30	70.6	27
Mixed culture	AC/BC (10)	Glucose	37	10	71	51
Mixed culture	Graphene (1.0)	Ethanol	35	12	25	53
Mixed culture	AC (10)	Acetate	35	20	78	54
Mixed culture	Graphene (0.12)	Glucose	35	12	51.4	55
Mixed culture	CC (2.5)	Ethanol	37	1	45	56
Heated sludge	CDMC (0.6)	Glucose	37	16	24.3	This study

Open Access Article. Published on 17 November 2020. Downloaded on 10/27/2025 2:31:16 PM.
This article is licensed under a Creative Commons Attribution-NonCommercial 3.0 Unported Licence.

Lee *et al.*[54] (78%), Tian *et al.*[55] (51.4%), Zhang *et al.*[51] (71%) and Zhao *et al.*[56] (45%) (Table 6). Nevertheless, there were obvious differences in the mixed culture, carbon source, OLR, fermentation temperature, and external carbon and mineral species, which impact biogas production. As described by Feng *et al.*,[57] anaerobic digestion is catalyzed by anaerobic mixed cultures with optimal metabolic pathways and operational conditions. Ambient (25 °C) and mesophilic (35 °C) conditions can achieve process stability and reduce thermal energy input.[57] As mentioned above, carbon matrix composites have been extensively studied for the generation H_2 and CH_4. However, the high cost and energy consumption of commercial carbon materials make them less economically attractive on an industrial scale. In addition, bioH_2 and CH_4 generation are generally achieved in two-phase bioreactors that are not easy to operate. Nonetheless, H_2 is a clean fuel and is widely applied in fuel cells, and its volumetric energy content (10.88 MJ m^{-3}) is much lower than that of CH_4 (36 MJ m^{-3}). In particular, considering the costs of H_2 transportation and storage, the application field of H_2 will likely be restricted in the near future. Therefore, compared to the two-phase process, the one-reactor approach to H_2 and CH_4 production has more advantages in terms of process, gas yield and costs than existing biotechnologies, which underscores the sustainability of anaerobic digestion. Therefore, the carbon materials have been playing vital roles in environmental application and energy generation.[58]

Fe and Co synergies on H_2 and CH_4 production

Microbial immobilization can be achieved by the colonization of microbial cells on the surface of. CDMC could also enrich Fe^{3+}-reducing microbes that could deploy different substrates and take part in the degradation of complex organic compounds the dissimilatory Fe reduction.[6] Simultaneously, Fe^{3+} converted into Fe^{2+}, which promoted Fe-hydrogenase activity increased IET rate from NADH to [Fe–Fe] hydrogenases, thereby increasing H_2 yield (Fig. 6).[6,17] CDMC also had an affinity for electrons, which further facilitated reduction of protons to H_2. Co^{2+} could release into liquid phase due to the acid condition caused by H_2 bioevolution, which was associated with some vitamins (*e.g.*, B_{12}), which played an important role in methanogenesis (Fig. 6). Both Fe^{2+} and Co^{2+} contributed to the CDMC buffering capacity, which provided suitable solution pH range (6.8–7.2) for subsequent methanogenesis. In addition, once CDMC was added into the anaerobic reactors, many *Geobacter* and *Methanosaeta* species on the surface of BC would be observed, which could participate in DIET process.[35]

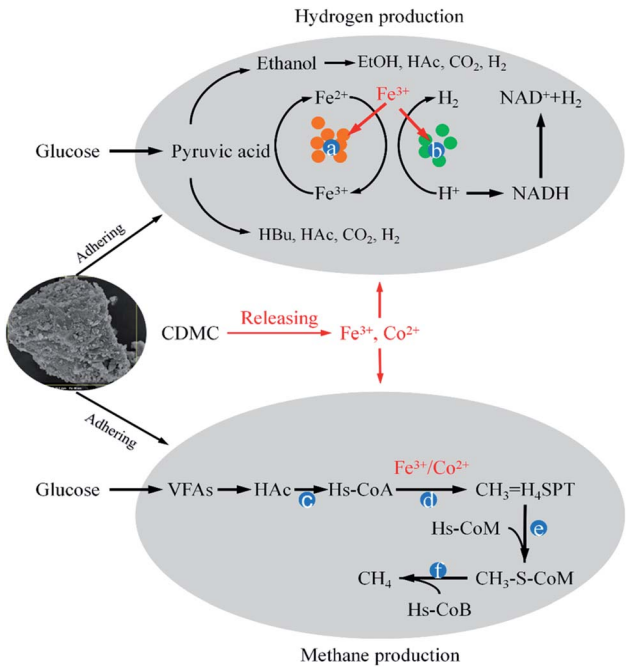

Fig. 6 The possible mechanisms of hydrogen and methane evolution enhanced by CDMC from glucose degradation: (a) ferredoxin; (b) hydrogenase; (c) acetyl coenzyme A synthetase; (d) carbon monoxide dehydrogenase (CODH); (e) methenyl tetrahydromethanopterin: coenzyme M methyltransferase; (f) methyl-coenzyme M reductase.

Conclusions

The CDMC composite was prepared and subsequently employed to boost bioH_2 production followed by CH_4 generation in one reactor. The CDMC (600 mg L^{-1}) group obtained the highest yields of 176 mL H_2 per g glucose and 358 mL CH_4 per g glucose. The findings indicated that CDMC obviously boosted H_2 and CH_4 yields by offering Fe^{3+} and Co^{2+} for glucose conversion, culture growth and many active sites and channels for electron transfer. The results also demonstrated that a one-pot approach to bioH_2 and CH_4 production is technically, economically, and environmentally sustainable.

Conflicts of interest

There are no conflicts to declare.

Acknowledgements

This work was supported by the Natural Science Foundation of Shandong Province (ZR2016EEM33).

References

1 H. T. Vu and B. Min, *Int. J. Hydrogen Energy*, 2019, **44**(14), 7574–7582.
2 I. Satar, W. R. W. Daud, B. H. Kim, M. R. Somalu and M. Ghasemi, *Energy*, 2017, **139**, 1188–1196.
3 A. E. Hosseini and M. A. Wahid, *Renewable Sustainable Energy Rev.*, 2016, **57**, 850–866.
4 M. A. Latif, C. M. Mehta and D. J. Batstone, *Water Res.*, 2017, **113**, 42–49.
5 G. Yang and G. Wang, *Renewable Sustainable Energy Rev.*, 2018, **95**, 130–146.
6 J. Zhang, W. Zhao, H. Zhang, Z. Wang and L. Zang, *Bioresour. Technol.*, 2018, **266**, 555–567.
7 A. Mostafa, A. El-Dissouky, A. Fawzy, A. Farghaly, P. Peu, P. Dabert, S. L. Roux and A. Tawfik, *Bioresour. Technol.*, 2016, **216**, 520–528.

Open Access Article. Published on 17 November 2020. Downloaded on 10/27/2025 2:31:16 PM.
This article is licensed under a Creative Commons Attribution-NonCommercial 3.0 Unported Licence.

8 A. Ali, R. B. Mahar, R. A. Soomro and S. T. H. Sherazi, *Energy Sources, Part A*, 2017, **39**(16), 1815–1822.
9 S. N. Malik, V. Pugalenthi, A. N. Vaidya, P. C. Ghosh and S. N. Mudliar, *Energy Procedia*, 2014, **54**, 417–430.
10 T. Seelert, D. Ghosh and V. Yargeau, *Appl. Microbiol. Biotechnol.*, 2015, **99**, 4107–4116.
11 H. Han, M. Cui, L. Wei, H. Yang and J. Shen, *Bioresour. Technol.*, 2011, **102**, 7903–7909.
12 K. S. Novoselov, V. I. Fal'Ko, L. Colombo, P. R. Gellert, M. G. Schwab and K. Kim, *Nature*, 2012, **490**, 192–200.
13 J. Gustavsson, S. S. Yekta, C. Sundberg, A. Karlsson, J. Ejlertsson, U. Skyllberg and B. H. Svensson, *Appl. Energy*, 2013, **112**, 473–477.
14 Q. Wei, W. Zhang, J. Guo, S. Wu, T. Tan, F. Wang and R. Dong, *Chemosphere*, 2014, **117**(1), 477–485.
15 J. Zhang, C. Fan, W. Zhao and L. Zang, *Int. J. Hydrogen Energy*, 2019, **44**(49), 26920–26932.
16 A. Z. Issah, T. Kabera and F. Kemausuor, *Biomass Bioenergy*, 2020, **133**, 105449.
17 Y. Zhang and J. Shen, *Int. J. Hydrogen Energy*, 2007, **32**(1), 17–23.
18 L. Zhang, L. Zhang and D. Li, *Int. J. Hydrogen Energy*, 2015, **40**(36), 12201–12208.
19 APHA, *Standard methods for the examination of water and wastewater*, American Public Health Association, Washington DC, 2005.
20 A. Asfaram, M. Ghaedi, S. Hajati, A. Goudarzi and E. A. Dil, *Ultrason. Sonochem.*, 2017, **34**, 1–12.
21 S. Menchaca-Nal, C. L. Londoño-Calderón, P. Cerrutti, M. L. Foresti, L. Pampillo, V. Bilovol, R. Candal and R. Martínez-García, *Carbohydr. Polym.*, 2016, **137**, 726–731.
22 J. Zhang, C. Fan, H. Zhang, Z. Wang, J. Zhang and M. Song, *Int. J. Hydrogen Energy*, 2018, **43**, 8729–8738.
23 D. M. F. Lima, W. K. M. Moreira and M. Zaiat, *Int. J. Hydrogen Energy*, 2013, **38**(35), 15074–15083.
24 X. Jia, Y. Wang, L. Ren, M. Li, R. Tang, Y. Jiang and J. Hou, *Int. J. Hydrogen Energy*, 2019, **44**(57), 30000–30013.
25 E. Abdelsalam, M. Samer, Y. A. Attia, M. A. Abdel-Hadi, H. E. Hassan and Y. Badr, *Renewable Energy*, 2016, **87**, 592–598.
26 Y. Chen, J. J. Cheng and K. S. Creamer, *Bioresour. Technol.*, 2008, **99**, 4044–4064.
27 C. Luo, F. Lü, L. Shao and P. He, *Water Res.*, 2015, **68**, 710–718.
28 N. M. S. Sunyoto, m. Zhu, Z. Zhang and D. Zhang, *Bioresour. Technol.*, 2016, **219**, 29–36.
29 Y. Shen, J. L. Linville, P. A. A. Ignacio-de Leon, R. P. Schoene and M. Urgun-Demirtas, *J. Cleaner Prod.*, 2016, **135**, 1054–1064.
30 C. E. G. Camacho, F. I. Romano and B. Ruggeri, *Energy*, 2018, **159**, 525–533.
31 R. Lin, J. Cheng, L. Ding, W. Song, M. Liu, J. Zhou and K. Cen, *Bioresour. Technol.*, 2016, **207**, 213–219.
32 S. Mohan, G. Mohanakrishna, S. Reddy, B. Raju, K. Rao and P. Sarma, *Int. J. Hydrogen Energy*, 2008, **33**, 6133–6142.
33 X. J. Zheng and H. Q. Yu, *Appl. Biochem. Biotechnol., Part A*, 2004, **112**, 79–90.
34 A. E. Rotaru, P. M. Shrestha, F. Liu, M. Shrestha, D. Shrestha, M. Embree, K. Zengler, C. Wardman, K. P. Nevin and D. R. Lovley, *Energy Environ. Sci.*, 2014, **7**, 408–415.
35 Z. Zhao, Y. Zhang, Q. Yu, Y. Dang, Y. Li and X. Quan, *Water Res.*, 2016, **102**, 475–484.
36 X. Chen, H. Yuan, D. Zou, Y. Liu, B. Zhu, A. Chufo, M. Jaffar and X. Li, *Chem. Eng. J.*, 2015, **273**, 254–260.
37 J. Ye, A. Hu, G. Ren, M. Chen, J. Tang, P. Zhang, S. Zhou and Z. He, *Water Res.*, 2018, **134**, 54–62.
38 J. Pan, J. Ma, L. Zhai and H. Liu, *J. Cleaner Prod.*, 2019, **240**, 118178.
39 B. Yang, H. Xu, Y. Liu, F. Li, X. Song, Z. Wang and W. Sand, *Chem. Eng. J.*, 2020, **383**, 123211.
40 Z. Zhao, J. Wang, Y. Li, T. Zhu, Q. Yu, T. Wang, S. Liang and Y. Zhang, *Water Res.*, 2020, **171**, 115425.
41 L. Guo, X. M. Li, G. M. Zeng and Y. Zhou, *Energy*, 2010, **35**(9), 3557–3662.
42 C. Mamimin, P. Prasertsan, P. Kongjan and S. Thong, *Electron. J. Biotechnol.*, 2017, **29**, 78–85.
43 E. E. Roden, A. Kappler, I. Bauer, J. Jiang, A. Paul, R. Stoesser, H. Konishi and H. Xu, *Nat. Geosci.*, 2010, **3**, 417–421.
44 B. R. Sreelekshmy, R. Basheer, S. Sivaraman, V. Vasudevan, L. Elias and S. M. A. Shibli, *J. Mater. Chem. A*, 2020, **8**, 6041–6056.
45 N. Duan, D. Zhang, B. Khoshnevisan, P. G. Kougias, L. Treu, Z. Liu, C. Lin, H. Liu, Y. Zhang and I. Angelidaki, *J. Cleaner Prod.*, 2020, **256**, 120414.
46 C. Zhang, X. Kang, N. Liang and A. Abdullah, *Energy Fuels*, 2017, **31**(11), 12217–12222.
47 C. C. Chen, C. Y. Lin and M. C. Lin, *Appl. Microbiol. Biotechnol.*, 2002, **58**, 224–228.
48 M. A. De la Rubia, V. Riau, F. Raposo and R. Borja, *Crit. Rev. Biotechnol.*, 2013, **33**, 448–460.
49 J. H. Park, H. K. Kang, K. H. Park and H. D. Park, *Bioresour. Technol.*, 2018, **254**, 300–311.
50 M. Zhang, G. Li, Y. Wang and C. Yang, *RSC Adv.*, 2019, **9**, 42375.
51 Z. Zhang, K. Y. Show, J. H. Tay, D. Liang and D. Lee, *Int. J. Hydrogen Energy*, 2008, **33**(5), 1559–1564.
52 J. Zhang, C. Fan and L. Zang, *Bioresour. Technol.*, 2017, **245**, 98–105.
53 R. Lin, J. Cheng, J. Zhang, J. Zhou, K. Cen and J. D. Murphy, *Bioresour. Technol.*, 2017, **239**, 345–352.
54 J. Y. Lee, S. H. Lee and H. D. Park, *Bioresour. Technol.*, 2016, **205**, 205–212.
55 T. Tian, S. Qiao, X. Li, M. Zhang and J. Zhou, *Bioresour. Technol.*, 2017, **224**, 41–47.
56 Z. Zhao, Y. Zhang, T. L. Woodard, K. P. Nevin and D. R. Lovley, *Bioresour. Technol.*, 2015, **191**, 140–145.
57 Q. Feng, Y. C. Song, D. H. Kim, M. S. Kim and D. H. Kim, *Int. J. Hydrogen Energy*, 2019, **44**(4), 2170–2179.
58 Q. Chen, X. Tan, Y. Liu, S. Liu, M. Li, Y. Gu, P. Zhang, S. Ye, Z. Yang and Y. Yang, *J. Mater. Chem. A*, 2020, **8**(12), 5773–5811.